35th International Electric Vehicle Symposium and Exhibition (EVS35)
Oslo, Norway, June 11-15, 2022

Electric Drivetrain Optimization for 48V Urban Vehicles

Dai-Duong Tran[a,b*], Amin Ghadirzadeh[a,b], Lamberto Salvan[c], Martin Brüll[d], Armin Hollstein[d], Róbinson Medina[e], Nikos Avramis[e], Steven Wilkins[e], Mohamed El Baghdadi[a,b], Omar Hegazy[a,b]

[a] *Vrije Universiteit Brussel, Pleinlaan 2, 1050 Brussels, Belgium*
[b] *Flanders Make, Flanders Make, 3001 Heverlee, Belgium*
[c] *Alkè, Via Cile 5, 35127 Padova, Italy*
[d] *Vitesco Technologies GmbH, Postfach 20 02 30, D-93061 Regensburg*
[e] *TNO, Powertrains Department, P.O. Box 756, 5700 AT, Helmond, The Netherlands*

* Corresponding author: dai-duong.tran@vub.be

Summary
This paper presents an optimization framework to determine the optimal sizing of main drivetrain components in a 48V battery electric vehicle applied for urban freight transport applications under a European project, namely URBANIZED. An evolutionary algorithm, NSGA-II, is adopted to solve a multi-objective optimization problem, which is formulated for the energy consumption and drivetrain cost of the vehicle. To evaluate the contradictory objective functions, a forward-facing and scalable vehicle model is developed for the integration into the optimization sizing loop considering different transport assignments. Comparative simulation results between optimized and baseline vehicles are provided and analyzed.

Keywords: NSGA-II, genetic algorithm, drivetrain optimization, last delivery, urban freight transport vehicle

1 Introduction

Urban freight transport (UFT) comprises five main market sectors: (*i*) retail (including e-commerce), (*ii*) express/couriers/post, (*iii*) hotel/restaurant/catering (HoReCa), (*iv*) construction, and (*v*) waste collection[1]. The negative emission-related impacts from UFT are expected to become even worse for the first three sectors. Due to their rapid growth when coupled with the raising (on-demand) last-mile deliveries and services, more and more goods will move into, out and within urban and suburban areas from urban consolidation centers and industrial areas around urban boundaries [2]. To cope with the problem, a European project called URBANIZED has been conducted with the wide adoption of zero-emission solutions such as battery electric vehicles (BEVs) [3]. This can introduce new generations of vehicle designs to the market, purpose-built solutions that meet the specific requirements of the changing nature of urban freight operations, and more sustainable logistics. Figure 1(a) shows an urban delivery vehicle (UFT N1 category) using BEV technology with a modularity concept, which means that one vehicle can handle at least four cargo bodies [4]. Easily swappable multi-purpose modular cargo bodies can be adaptable to fluctuating demands, which can reduce fleet size and operational costs. A high performance and flexible e-drivetrain platform based on component's right-sizing (see Figure 1(b)), integration and modularization will need to be designed to meet all vehicle performance requirements.

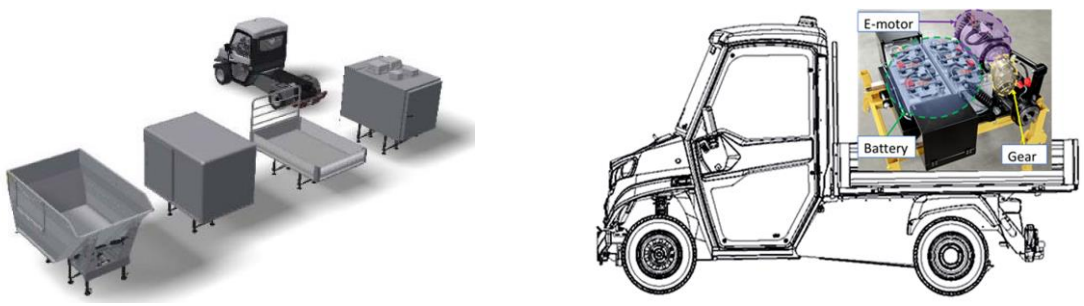

(a) (b)

Figure 1. (a) Urban delivery vehicles (N1 category) using BEV technology for multiple cargo bodies, (b) main drivetrain components need to be designed for 'one size fits all'.

Owning a holistic approach, a three-stage design procedure (see Figure 2) has been widely adopted to optimize sequentially the topology, the component sizing, and the controller for a BEV. Regarding the first stage 'topology optimization', several comparative studies evaluated different drivetrain configurations for a given vehicle mission profile through literature. Various topologies can be considered specifically for BEV drivetrains such as single-motor single-axle (single e-motor driving a single axle with a fixed gear ratio), double-motor double-axle (separate motors – each with fixed gear ratio - for the front axle and the rear axle), in-wheel-motors on a single-axle, in-wheel-motors double-axle (four-wheel-drive) [5]–[8]. Once drivetrain topology is fixed, at the second stage, specific technologies used for main components need to be selected properly to trade-off between drivetrain cost and vehicle performance [9]. For example, the electric motor (EM) technologies can be selected as induction motor (IM), permanent magnet synchronous motor (PMSM), and switched reluctance motor (SRM). Likewise, battery technologies depend on the cell chemistries such as–nickel-manganese-cobalt (NMC), lithium-iron-phosphate (LFP), lithium-titanium-oxide (LTO), etc. Regarding the control design, BEVs typically require sophisticated energy management strategies (EMSs) to maximize the drivetrain efficiency or minimize the vehicle energy consumption while satisfying relevant physical constraints. These strategies can consist of multi-level multi-layer EMSs. For instance, at the vehicle level, a single layer EMS can optimize the vehicle speed (i.e. eco-driving) while another EMS can optimize the thermal management (i.e. eco-comfort in the cabin). However, the topics of control design and EMS implementation are out of the scope of this study. This paper will deal with only the 'sizing optimization' methodology in the second stage. The drivetrain topology, component technologies, and controller type have been pre-selected and considered to be fixed for the component sizing optimization loop.

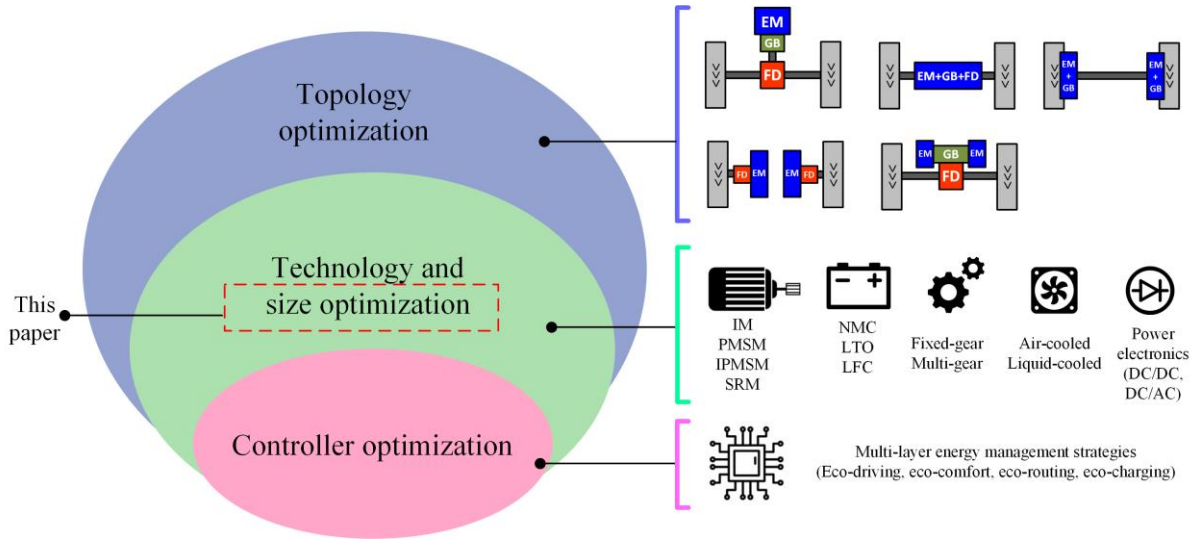

Figure 2. Vehicle design procedure.

For sizing drivetrain components, different optimization algorithms can be utilized for plug-in hybrid electric vehicles (PHEVs) and BEVs. In [10], a global search method has been used to find the optimal sizing for battery and fuel-cell of a vehicle. Convex programming has been widely adopted for sizing a battery in PHEV [11], dual-motor driven electric powertrain [12]. Other methods, known as heuristic algorithms, such as particle swarm algorithm [13], self-adaptive differential evolution [14], and genetic algorithm [15], [16], have been widely used for sizing drivetrain components. Among them, the non-dominated sorting genetic algorithm II (NSGA-II) is demonstrated to effectively solve multi-objective optimization problems [5], [17]. From previous analyses, no existing papers can be found for component sizing for the 48V BEV N1 type. The contribution of this paper is to develop an optimization framework to find an optimal drivetrain, which is a trade-off between a 'one size fits all' and a 'design for purpose' objective, thanks to modular vehicle architectures. A "design for purpose" objective is guaranteed by including typical mission-profiles drive cycles of the use cases where the vehicle is to be used. A "one size fits all" objective is guaranteed using modular vehicle architectures which apply to several use cases.

This paper is organized as follows. After the introduction, section 2 presents the drivetrain configuration selected for this study. Section 3 explains the principle of a multi-objective optimization framework

developed based on a forward-facing and scalable vehicle model. Section 4 shows simulation results for vehicle performances and component sizing optimization. Section 5 concludes the paper.

2 Vehicle Drivetrain Topology and Mission Profiles

In this study, the drivetrain topology has been selected as a rear-drive configuration (see Figure 3(a)) that includes a single PMSM EM (multi-phase motor) at the rear-axle, gearbox (GB) 1-fixed ratio, 48VLFP battery This paper focuses on a design methodology to obtain the right sizing for those main drivetrain components. Figure 3(b) shows the 3D CAD design for the rear-drive axle and e-motor integration.

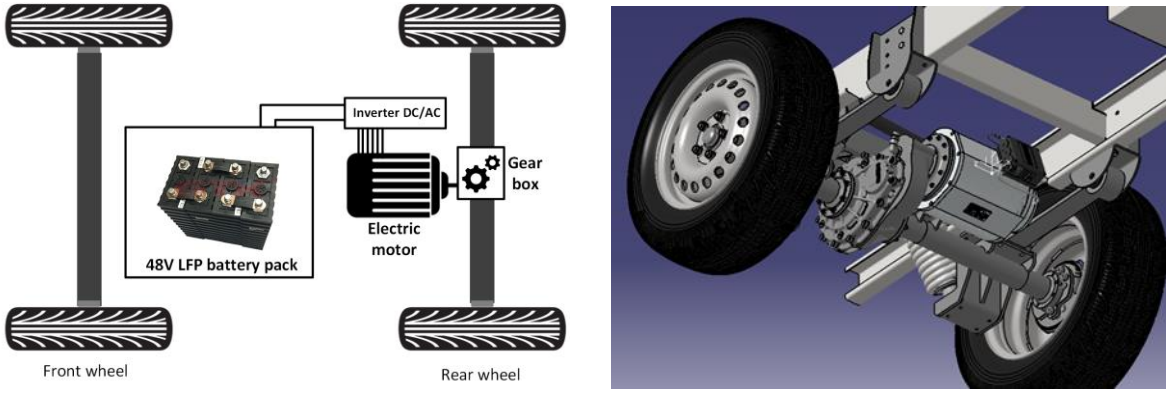

(a) (b)

Figure 3.(a) rear-drive e-drivetrain block diagram, (b) rear-drive axle and e-motor integration.

The sizes of drivetrain components are dependent on the transport mission profiles or driving cycles that the vehicle is assigned to work for. Due to the nature of the expected routes (frequent stops for parcel/product deliveries), a standard drive cycle (e.g., WLTP, SORT) could not accurately capture the expected driving behavior. In this work, a mission profile generation (MPG) tool has been developed to create the vehicle driving cycles used typically in two use-cases (UCs) for the urban vehicles. UC1 is the HoReCa and on-demand emergency services and UC2 is the last-mile delivery of retail, courier, and post. In this study, two of the most challenging driving cycles (maximum speed 70km/h) have been selected for vehicle simulation and optimization. One driving cycle called Coffee Island (COI) represents UC1 (see Figure 4), whilst another one called BPOST is for UC2 (see Figure 5). Notice that the drive cycle of Figure 5 shows significantly more stops and relatively fewer high-speed moments than the drive cycle of Figure 4. This is because of the nature of the vehicle operations: the former drive cycle requires the vehicle to constantly stop in a relatively small neighborhood to deliver small packages (i.e., post), while the latter drive cycle corresponds to larger deliveries over a wider range of neighborhoods for Horeca. Other vehicle mission profiles can be found in Appendix.

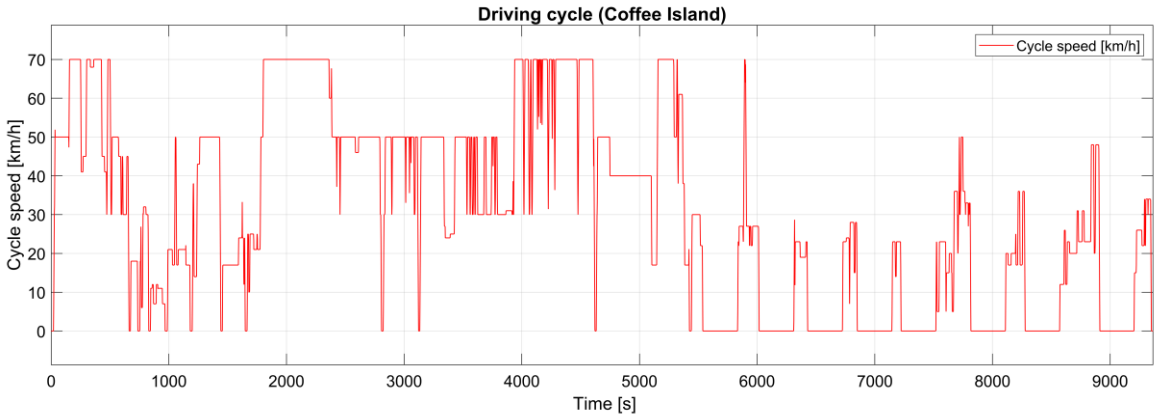

Figure 4. Driving cycle for HoReCa and on-demand emergency services.

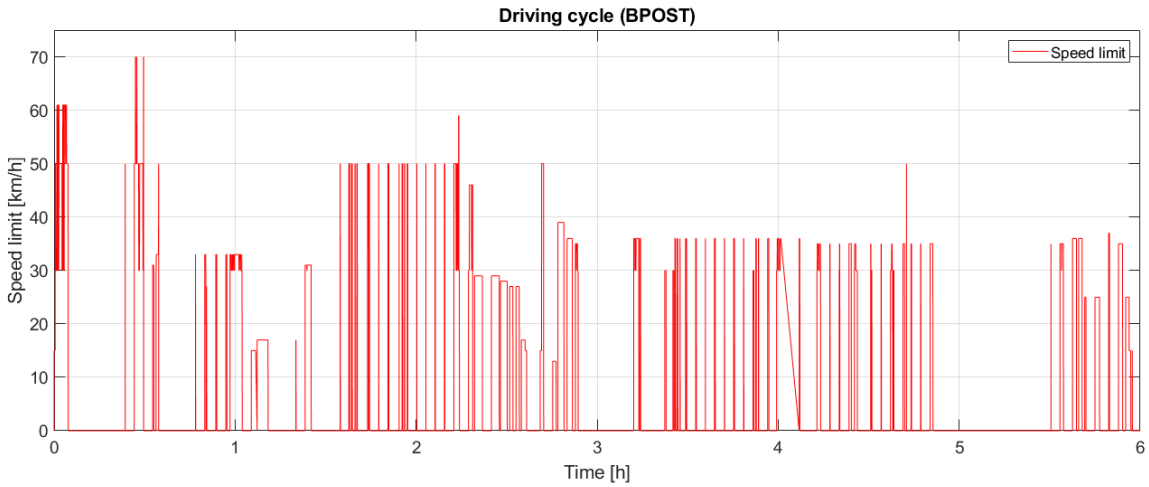

Figure 5. Driving cycle for last-mile delivery of retail, courier and post.

3 Optimization Framework

3.1 Multi-objective Optimization Problem Formulation

In this study, the boundaries of e-motor power and battery capacity need to be optimized to minimize two contradictory objectives: battery energy consumption and drivetrain cost minimization. A mathematical formulation for a multi-objective optimization problem is given as follows.

$$\begin{aligned} &\textit{Minimize } (\text{Obj1}(\mathbf{X_D}), \text{Obj2}(\mathbf{X_D})) \\ &\textit{Subject to } \{\text{vehicle performance requirements}\} \end{aligned} \tag{1}$$

Obj1$\mathbf{(X_D)}$ is battery energy consumption [kWh/km], Obj2$\mathbf{(X_D)}$ is drivetrain cost [€]. A design vector $\mathbf{X_D}$=(P_{em}, E_{bat}) includes two variables, maximum e-motor power $P_{em}[kW]$ and battery capacity $E_{bat}[kWh]$, respectively. It is assumed that the GB ratio is fixed at 10.39:1. The design constraints are the vehicle performance requirements shown in Table 1. The energy consumption Obj1$\mathbf{(X_D)}$ can be determined from a vehicle simulation in Matlab/Simulink developed based on a forward-facing model (Section 3.2). The drivetrain cost Obj2$\mathbf{(X_D)}$ can be calculated analytically using assumptions for the components cost.

Table 1. Vehicle performance requirements.

Performance requirement	Description
Vehicle acceleration	The vehicle shall have a powertrain able to accelerate on flat regular road, no wind, with 205/65R15 tires: - From standstill to 50km/h within 15sec at empty payload - From standstill to 70km/h within 25sec at empty payload
Maximum vehicle speed	The vehicle shall have a powertrain able to deliver a top speed of: - 70km/h on flat road, no wind - 50km/h on flat road, no wind
Maximum road slope	The fully loaded vehicle shall deal with at least 18% slopes without trailer
Maximum road slope with trailer	The fully loaded vehicle shall deal with at least 12% slopes when coupled with a trailer
Range	The vehicle shall attain a driving range of 100 km based on WLTP

To solve the multi-objective optimization problem above, non-dominated sorting genetic algorithm (NSGA-II) [18] has been employed in this study. In principle, the NSGA-II uses a Pareto-front hierarchy and adopts an elitism mechanism to retain the best solutions generated during the search. All design variables have been varied by the searching rules of NSGA-II during the optimization process. Therefore, the updated characteristics of design variables stored in the database can be fetched out to evaluate objective functions.

Figure 6 illustrates the principle of the optimization loop to search for the optimal values of component sizing.

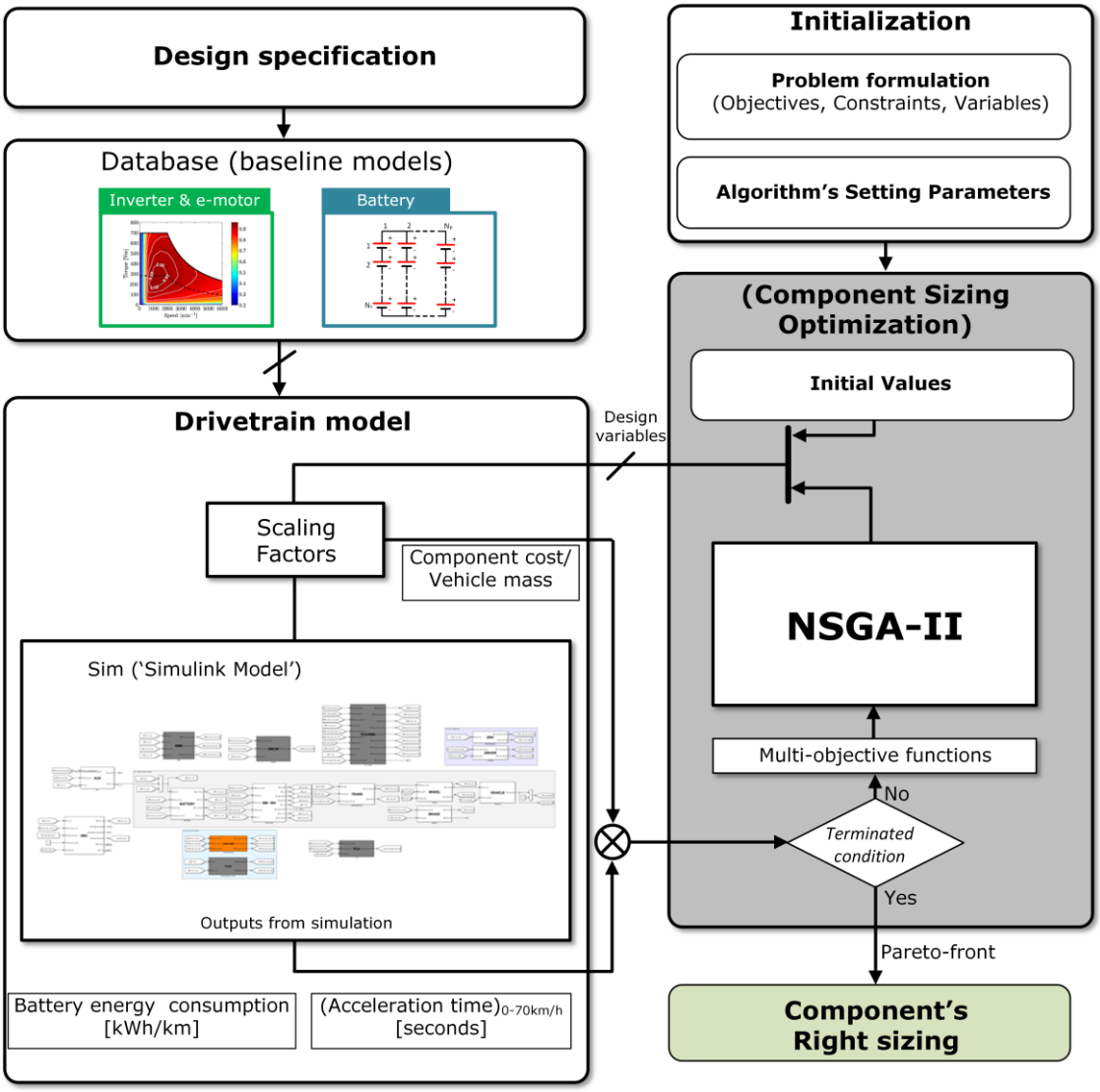

Figure 6. Optimization loop for component sizing.

The NSGA-II is terminated when the maximum generation is reached. A set of design solutions found is returned as the Pareto-front in which no other solutions are superior to those in its set when all objectives are considered. In other words, in the Pareto-front, each candidate solution can be considered equally good. A common post-processing approach is that the designer with their preference and design experience could select a compromised solution from amongst Pareto front solutions

3.2 Scalable Vehicle Modeling

As it can be seen in Figure 6, a vehicle simulation model is required to evaluate vehicle performance metrics such as acceleration time, electrical energy consumption, and battery SoC over a driving cycle. Therefore, an energy consumption model for the vehicle based on longitudinal dynamics and the forward-facing model has been developed in Matlab Simulink.

3.2.1 Electric Motor Model

The EM is represented by an efficiency map (see Figure 7) stored in a look-up table as a function of physical torque [Nm] and speed [rad/s]. The losses of the power electronics inverter (INV) are included in this efficiency map. It is assumed that the global losses of the EM and INV are independent of the battery voltage. The EM model can be resized by the optimization algorithm to create multiple power demands by adjusting

a scaling factor (s_{EM}).The scaling factor is the ratio between the newly updated power $P_{EM(scaled)}$ and a reference base power $P_{EM(base)}$. s_{EM} is presented in (3) where the maximum torques $\overline{T}_{EM(scaled)}$ of the scaled components are proportional to the maximum torques $\overline{T}_{EM(base)}$ of the base models.

$$s_{EM} = \frac{P_{EM(scaled)}}{P_{EM(base)}} \tag{2}$$

$$\overline{T}_{EM(scaled)} = s_{EM} \cdot \overline{T}_{EM(base)} \tag{3}$$

The EM is scaled up or down by only extending or shortening the torque axis on the efficiency map. The speed axis remains the same, and the efficiency map is extrapolated as required.

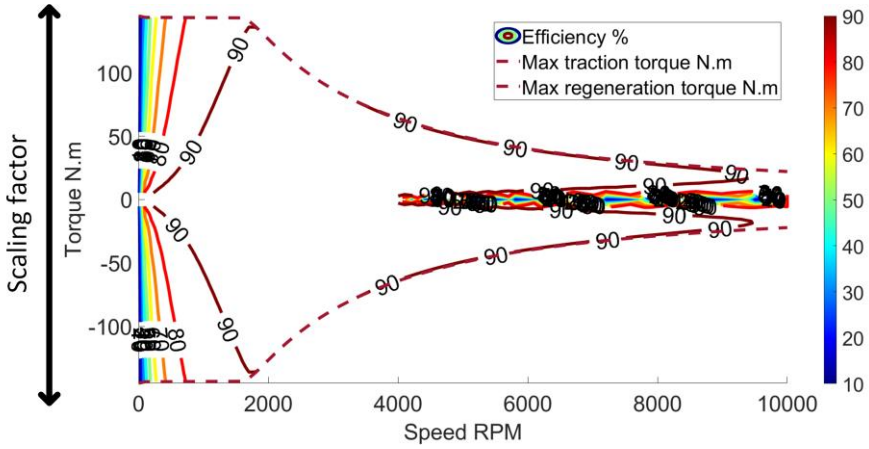

Figure 7. EM base maps for scalable model.

The electric power consumption of EM is calculated as (6).

$$\eta_{EM} = f(\omega_{EM}, \frac{T_{EM}}{s_{EM}}) \tag{4}$$

$$P_{EM(elec)} = w_{EM}(t) \cdot T_{EM}(t) \cdot \eta_{EM}^{-sign(T_{EM}(t))} \tag{5}$$

In which η_{EM} is the EM efficiency.

3.2.2 Battery Pack Model

The lithium-ion battery (LiB) pack comprises N_s cells in series and N_p strings in parallel as shown in Figure 8. The number of LiB cells in series is calculated properly to form the required terminal voltage of LiB pack. The number of strings in parallel is varied by the optimization algorithm.

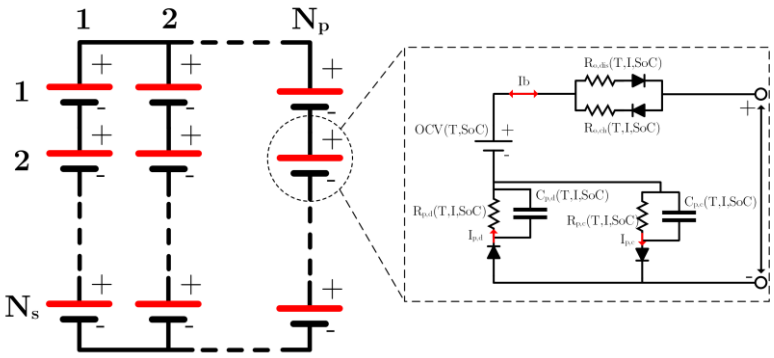

Figure 8. Battery pack configuration and battery cell equivalent model.

In this study, the model of battery cell is based on semi-empirical first order Thevenin equivalent circuit. The parameters of this model can be identified by using experimental data, which are stored in Simulink look-up tables [19]. As shown in Figure 8, this model takes into account two variable ohmic resistances ($R_{O,ch}$ and $R_{O,dis}$), two variable polarization RC circuits composed of two polarization resistances ($R_{p,c}$ and $R_{p,d}$) and two polarization capacitors ($C_{p,c}$ and $C_{p,d}$) and an open circuit voltage (OCV). The subindices ch and dis represent charging and discharging, respectively. The split-up of the components in charging and discharging takes the hysteresis into account. The model of the LiB captures the state of charge (SoC), current rate and operating temperature dependencies. This allows investigating the power behavior of the energy sources under different operating conditions.

3.2.3 Vehicle Longitudinal Model

To follow the reference speed requested by the driver, the traction force F_{tract} [N] in (6) at the wheels is required to drive the vehicle, which can be calculated as considering the rolling friction, aerodynamic friction, and slope resistance.

$$F_{tract}(t) = M_{veh}\left(c_r g\cos(\theta(t)) + g\sin(\theta(t)) + dv/dt\right) + \frac{1}{2}\rho A_{front} c_d v(t)^2 \quad (6)$$

The vehicle parameters and coefficients can be found Table 2. θ [rads] corresponds to the road grade while v [m/s] is the vehicle speed.

Table 2. Vehicle parameters.

ALKE ATX3 baseline vehicle	Parameter	Value	Unit
	Vehicle unladen mass	1200	kg
	GCW vehicle mass (driver + load + vehicle)	1600	kg
	Gravitational acceleration	9.81	m/s^2
	Rolling friction coefficient	0.01	-
	Aerodynamic drag coefficient	0.4	-
	Frontal area	2.5	m^2
	Air density	1.225	kg/m^3
	Wheel inertia	1	$kg.m^2$
	Wheel radius	0.32	m

3.2.4 Vehicle Mass Model

The vehicle mass (M_{veh}) has an impact in the vehicle performances such as energy consumption and acceleration performance. Since the sizing of design components are updated according to the optimization algorithm, the total mass of the vehicle is also changed and computed as below.

$$M_{veh} = M_{baseline} + m_{EM}.P_{EM} + m_{BAT}.E_{BAT} \quad (7)$$

Where, $M_{baseline}$: vehicle baseline mass; m_{EM} : mass density of electric motor [2.4 kg/kW]; m_{BAT} is battery mass density [6.25 kg/kWh]; E_{BAT} is battery capacity [kWh].

3.2.5 Drivetrain Cost Model

Regarding the component cost model, as design variables include battery size and e-motor power, the objective function of drivetrain cost ($€_{drivetrain} = €_{BAT} + €_{EM}$) is formulated as the sum of battery cost and EM cost. It is assumed a battery cost per kWh of [200€/kWh] and an e-motor cost per kW of [8.75€/kW] [20]. Other costs for chassis, vehicle body, gearbox remain unchanged for the optimization loop.

4 Simulation and Optimization Results

4.1 Baseline Vehicle Simulation Results

The developed vehicle model is used for the impact assessment of different component sizes on the vehicle performances. Figure 9 shows an overall simulation result of the vehicle using 25kW EM, 10.39:1 gear ratio, 20kWh 48V LFP battery. In this figure, the vehicle model uses as input a desired speed profile, generated by the MPG tool. The simulation model tracks the desired speed up to the maximum vehicle speed of 70km/h. To do so, a driver model actuates over acceleration and brake pedals, which in turn results in EM power and battery current. As shown in Figure 10, the vehicle simulation can also generate relevant information about the EM (e.g. torque, temperature, speed). Besides, other information such as the vehicle (e.g. wheel torques, acceleration, etc.) and the battery information (e.g., voltage, SoC, etc.) is used by the optimization algorithm to determine the optimal component sizing in the next subsection.

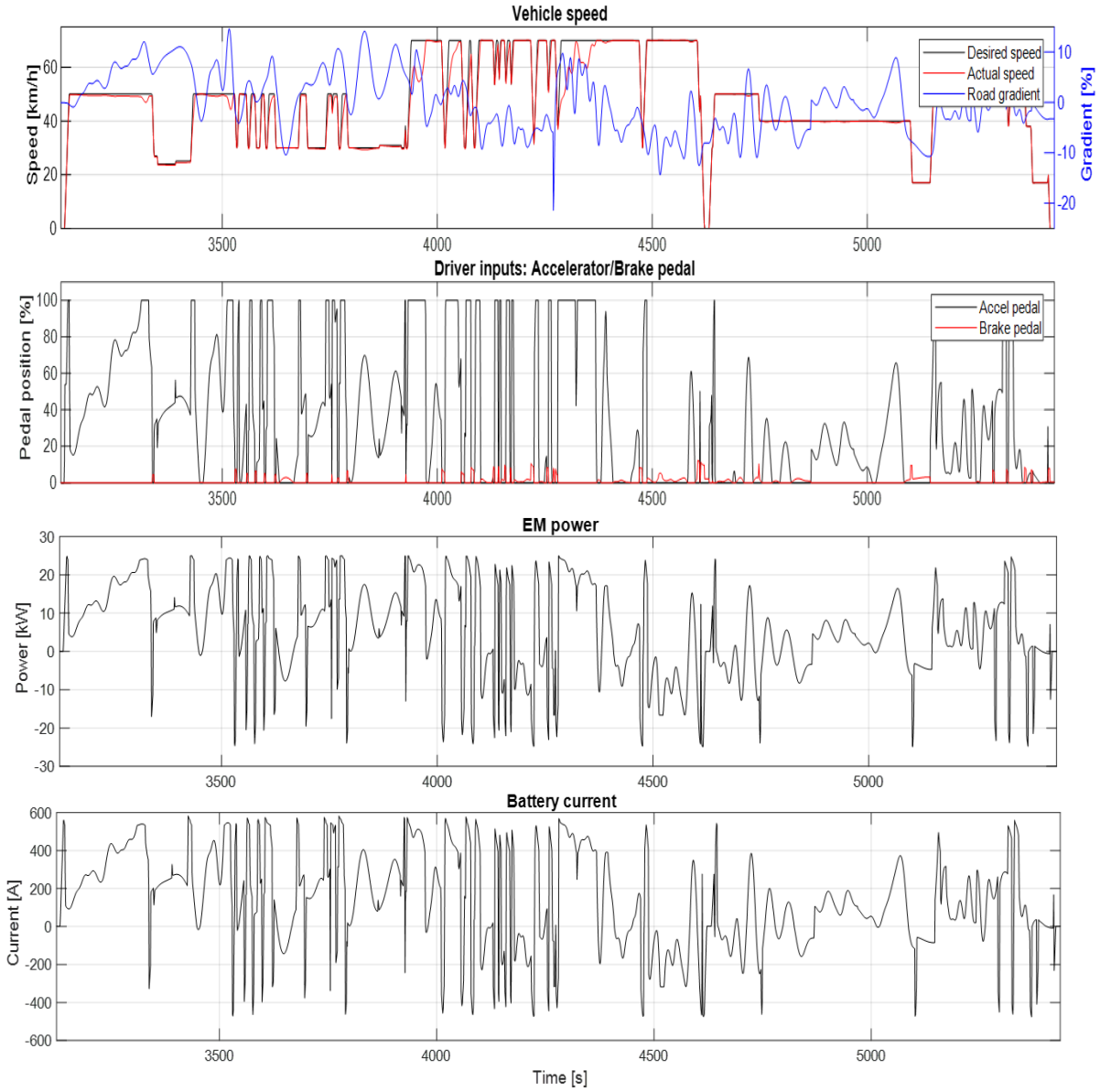

Figure 9. Overall simulation results.

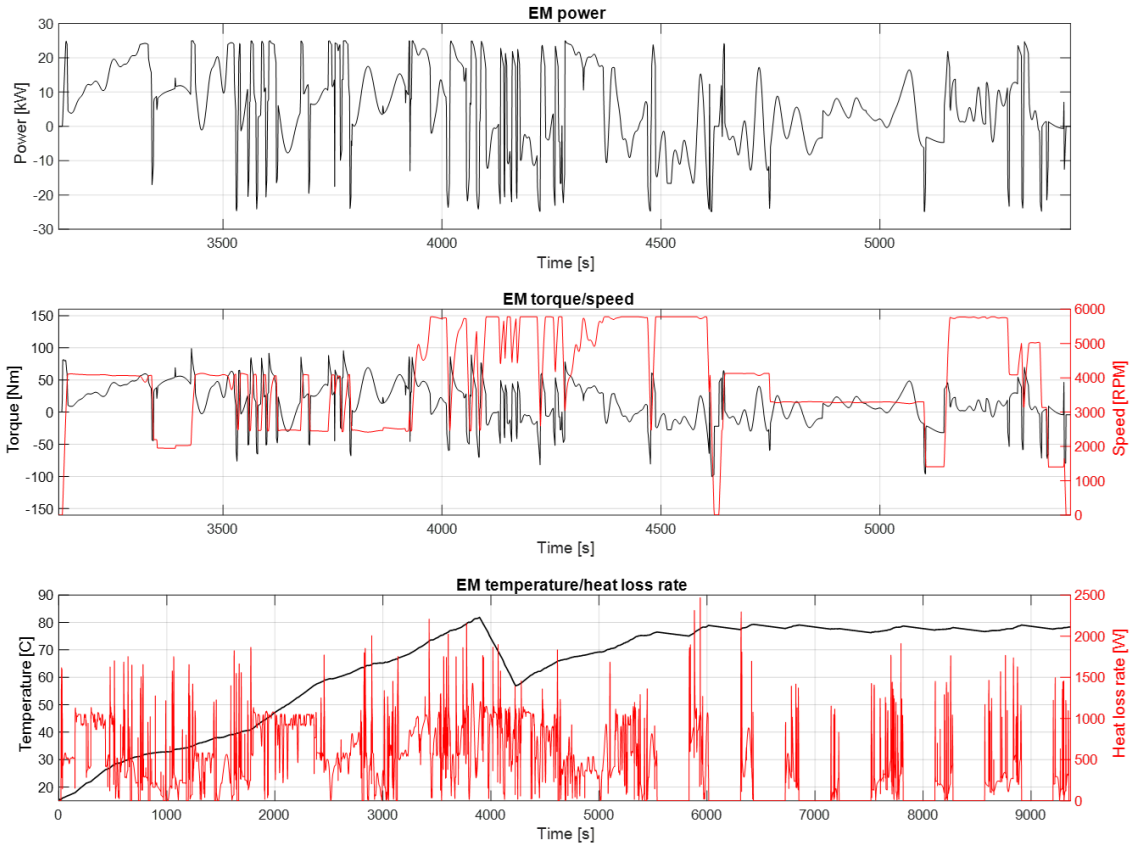

Figure 10. Simulation results of electric motor.

4.2 Component Sizing Optimization Results

Given the optimization problem formulated in (1), the settings of NSGA-II for two design variables and two objective functions are as follows: number of maximum generations = 10, population size = 20. The optimal solutions for component sizing need to be considered under two driving cycles in Figure 4 and Figure 5. Figure 11 shows Pareto front optimization solutions for the two use cases. The design variables converge to optimal solutions after 10 generations of NSGA-II. In the Pareto-front, each candidate solution can be considered equally good, meaning that no other solutions are superior to those in its set when all objectives are considered. A common post-processing approach is that the designer with their preference and design experience could select a compromised solution from amongst Pareto front solutions. One of practice widely used is that knee-point solutions from the Pareto-front can be considered as the preferred solution if there is no other preference. In this study, the optimal solution $X_D^* = [P_{em}^* = 35kW, E_{bat}^* = 20kWh]$ is found as the knee-point solution for both COI and BPOST as highlighted in Figure 11.

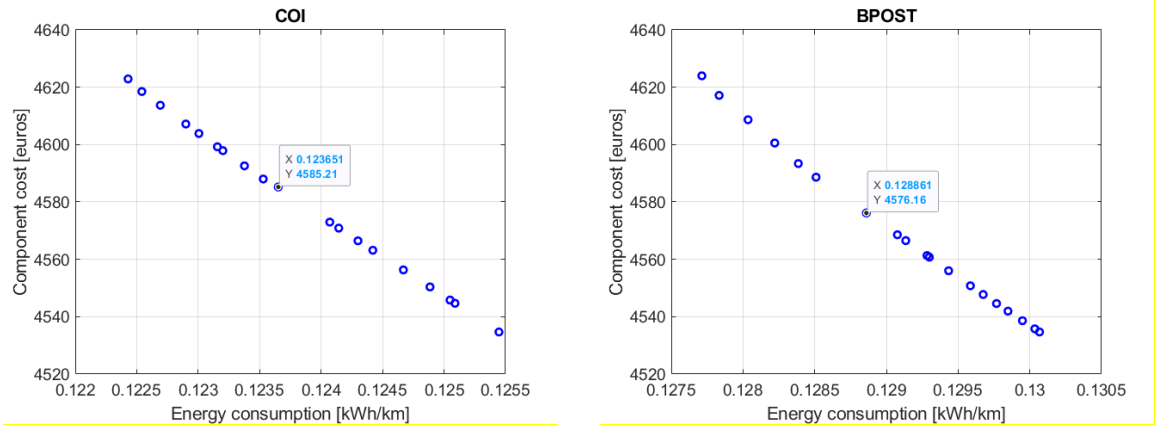

Figure 11. Pareto optimization results for (a) COI, (b) BPOST.

Table 3 shows the comparison between baseline vehicle and optimization results. The battery capacity is still the same whereas the e-motor's optimal sizing has been found at 35kW, which is increased by 40% compared to the e-motor sizing (25kW) in the baseline vehicle. As the optimal e-motor is bigger than the baseline one, the component cost of the optimal drivetrain is also slightly higher (+3.1%) than that of baseline vehicle. However, the energy consumption kWh/km of the optimal drivetrain can be lower than that of the baseline vehicle for both use-cases.

Table 3. Comparison between baseline vehicle and optimization results.

	Baseline vehicle (B)	**Optimization (O)**	**Δ = ((O-B)/B)*100%**
Battery capacity	20 kWh	20 kWh	ΔBAT=0
E-motor peak power	25 kW	35 kW	ΔEM = +40%
E-motor and battery cost	4447 €	4585 €	Δcost = +3.1%
Energy consumption (COI)	0.1256 kWh/km	0.1236 kWh/km	Δenergy(COI) = -1.6%
Energy consumption (BPOST)	0.1335 kWh/km	0.1288 kWh/km	Δenergy(BPO) = -3.5%

Figure 12 shows the comparison of vehicle acceleration from 0-70km/h with no payload. As can be seen, the optimized vehicle can reach 70km/h within 25s, which satisfies the requirements in Table 1. Figure 13 shows the vehicle speed considering the gradeability performance for the COI driving cycle during the 3900s-4000s when the vehicle needs to go up the maximum speed at a high road gradient. Compared to the baseline vehicle, the optimal vehicle can follow better the desired speed. Though the component mass and cost of the optimal drivetrain were increased, the vehicle performance requirements are fulfilled thanks to a bigger e-motor with higher torque at low speed.

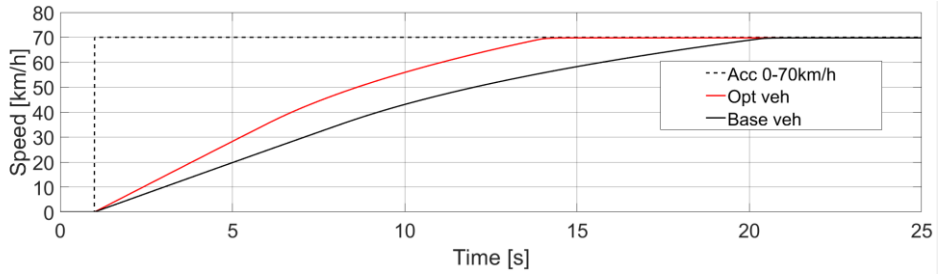

Figure 12. Comparison of acceleration performance between baseline and optimal drivetrain.

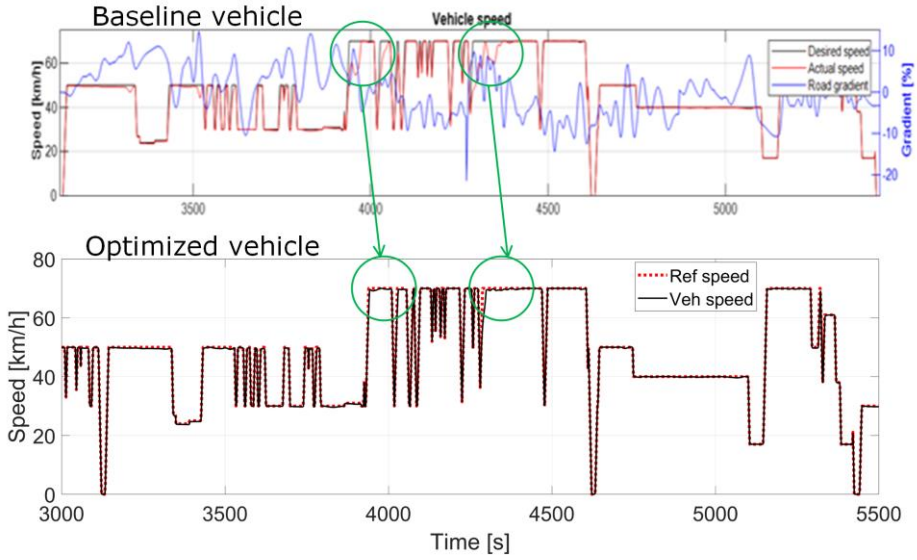

Figure 13. Comparison of gradeability performance between baseline and optimal drivetrain.

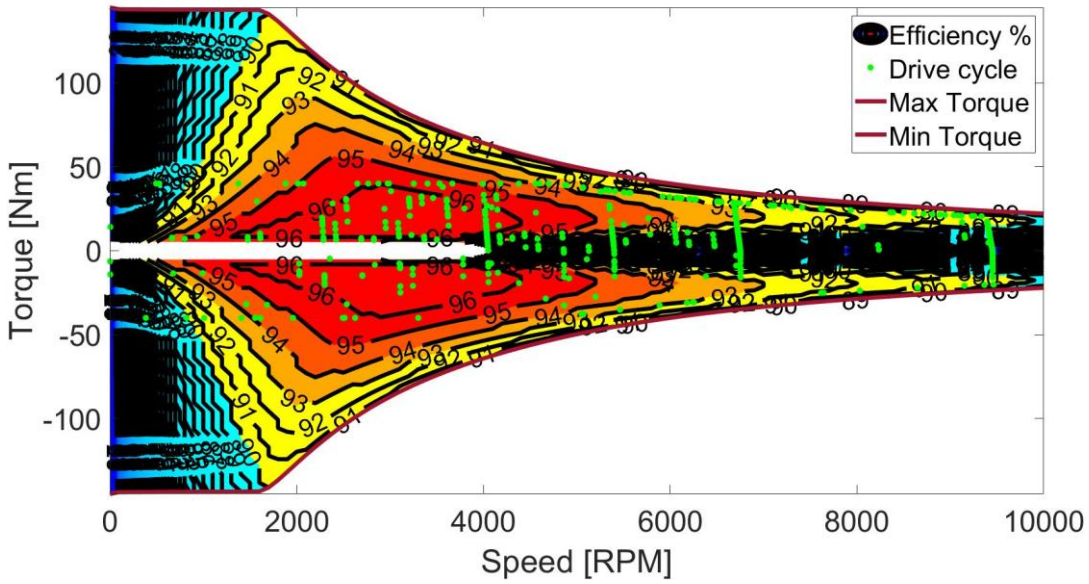

(a)

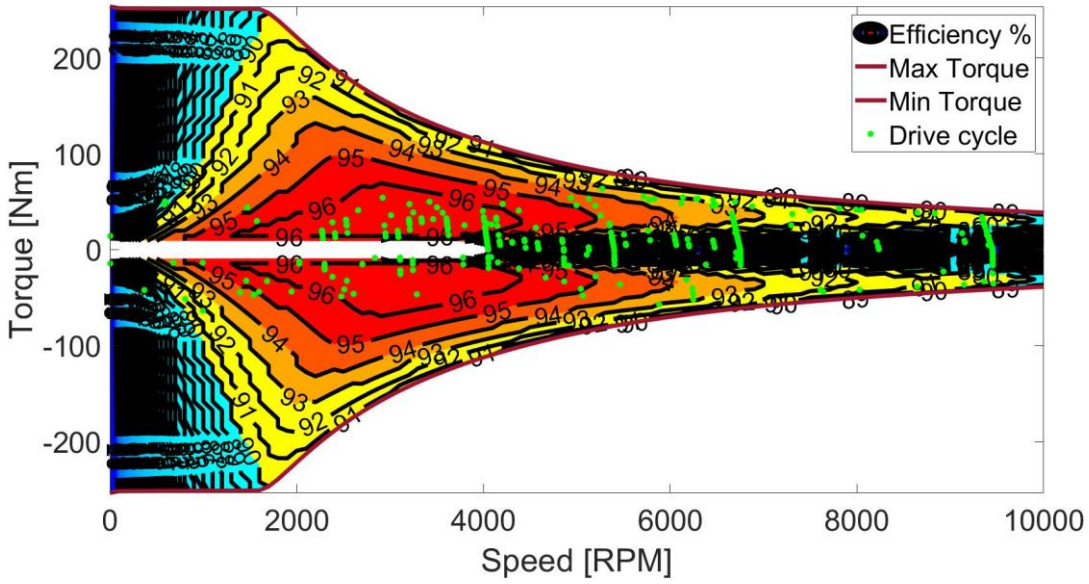

(b)

Figure 14. Operating points between (a) baseline EM and (b) optimal EM.

Figure 14 shows the comparison of operating points between the baseline (25kW) and optimal (35kW) electric motors. Considering the regeneration zone, the operating points of the optimal EM are switched from low-efficiency to high-efficiency points, resulting in more energy being recuperated for the battery. Therefore, the energy consumption of the optimal drivetrain can be lower than that of the baseline vehicle for both use-cases. Energy reduction is an important enabler to reduce further the operational cost for fleet management and the total cost of ownership in the long term over the vehicle lifetime.

5 Conclusions

This paper proposed an optimization framework to determine the optimal sizing of e-motor and battery for a 48V e-drivetrain utilized in urban vehicles. A forward-facing and scalable simulation model in Matlab/Simulink has been developed to evaluate virtually vehicle performances such as battery energy

consumption and drivetrain cost, which are the considered objective functions to be minimized. The evolutionary-based NSGA-II algorithm has been employed to solve the multi-objective functions considering different driving cycles representing the HoReCa, on-demand emergency services and last-mile delivery of retail, courier, and post. The simulation and optimization results showed that compared to the baseline vehicle, the optimized e-motor would need higher power (up to 35kW), increasing 40%, to cover the gradeability and acceleration requirements for the vehicle. It would lead to an increase (+3.1%) in the component cost, however, the energy consumption kWh/km of the optimized drivetrain can be reduced by 3.5% when compared to the baseline vehicle. Future work will include the gear ratio with multi-speed transmission and gearshift control strategy in the optimization loop.

Acknowledgments

This research has received funding from the European Union's Horizon 2020 research and innovation programme under grant agreement No 101006943, under the title of URBANIZED (https://urbanized.eu/).

Appendix

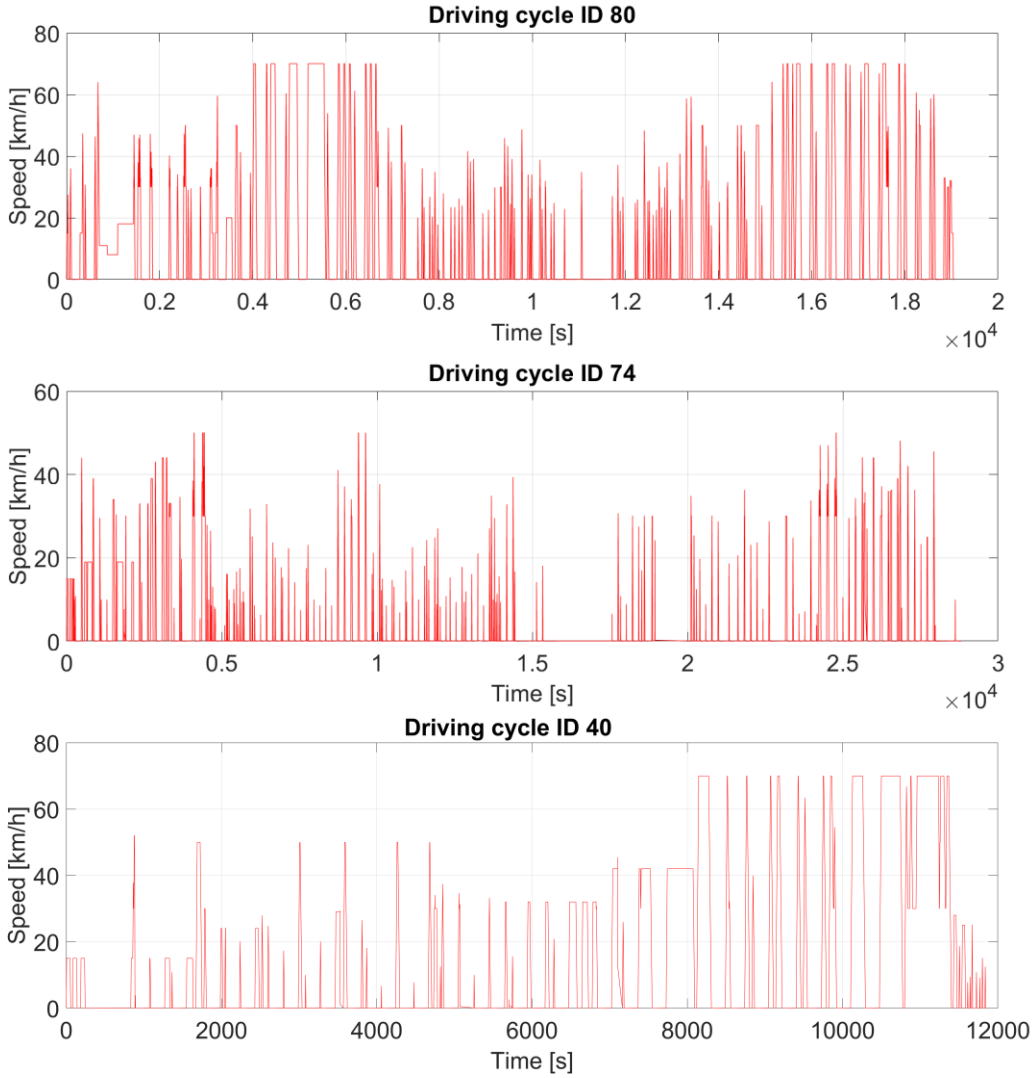

Figure 15. Other driving cycles generated from MPG tool.

References

[1] MDS Transmodal Limited, "DG MOVE European Commission: Study on Urban Freight Transport, FINAL REPORT," 2012. [Online]. Available: http://civitas.eu/sites/default/files/2012_ec_study_on_urban_freight_transport_0.pdf

[2] World Economic Forum, "The Future of the Last-Mile Ecosystem," *World Economic Forum*, no. January, pp. 1–26, 2020, [Online]. Available: https://www.weforum.org/reports/the-future-of-the-last-mile-ecosystem

[3] "Modular and Flexible Solutions for Urban-Sized Zero-Emissions Last-Mile Delivery and Services Vehicles." https://urbanized.eu/

[4] Alkè, "Alke' Electric Utility Vehicles." https://www.alke.com/

[5] P. Othaganont, F. Assadian, and D. J. Auger, "Multi-objective optimisation for battery electric vehicle powertrain topologies," *Proceedings of the Institution of Mechanical Engineers, Part D: Journal of Automobile Engineering*, vol. 231, no. 8, pp. 1046–1065, Jul. 2017, doi: 10.1177/0954407016671275.

[6] S. de Pinto *et al.*, "On the Comparison of 2- and 4-Wheel-Drive Electric Vehicle Layouts with Central Motors and Single- and 2-Speed Transmission Systems," *Energies (Basel)*, vol. 13, no. 13, p. 3328, Jun. 2020, doi: 10.3390/en13133328.

[7] S. Schumacher, S. Schmid, P. Wieser, R. Stetter, and M. Till, "Design, Simulation and Optimization of an Electrical Drive-Train," *Vehicles*, vol. 3, no. 3, pp. 390–405, Jul. 2021, doi: 10.3390/vehicles3030024.

[8] L. Zhang, L. Li, B. Qi, and J. Song, "Configuration Analysis and Performance Comparison of Drive Systems for Pure Electric Vehicle," in *SAE Technical Papers*, Apr. 2015, vol. 2015-April, no. April. doi: 10.4271/2015-01-1165.

[9] K. Wagh and P. Dhatrak, "A review on powertrain subsystems and charging technology in battery electric vehicles: Current and future trends," *Proceedings of the Institution of Mechanical Engineers, Part D: Journal of Automobile Engineering*, vol. 236, no. 4, pp. 479–496, Mar. 2022, doi: 10.1177/09544070211025906.

[10] L. Xu, C. D. Mueller, J. Li, M. Ouyang, and Z. Hu, "Multi-objective component sizing based on optimal energy management strategy of fuel cell electric vehicles," *Applied Energy*, vol. 157, pp. 664–674, Nov. 2015, doi: 10.1016/j.apenergy.2015.02.017.

[11] N. Murgovski, L. Johannesson, J. Sjöberg, and B. Egardt, "Component sizing of a plug-in hybrid electric powertrain via convex optimization," *Mechatronics*, vol. 22, no. 1, pp. 106–120, Feb. 2012, doi: 10.1016/j.mechatronics.2011.12.001.

[12] X. Hu, Y. Li, C. Lv, and Y. Liu, "Optimal Energy Management and Sizing of a Dual Motor-Driven Electric Powertrain," *IEEE Transactions on Power Electronics*, vol. 34, no. 8, pp. 7489–7501, Aug. 2019, doi: 10.1109/TPEL.2018.2879225.

[13] X. Zhou, D. Qin, and J. Hu, "Multi-objective optimization design and performance evaluation for plug-in hybrid electric vehicle powertrains," *Applied Energy*, vol. 208, no. 174, pp. 1608–1625, 2017, doi: 10.1016/j.apenergy.2017.08.201.

[14] L. Wu, Y. Wang, X. Yuan, and Z. Chen, "Multiobjective optimization of HEV fuel economy and emissions using the self-adaptive differential evolution algorithm," *IEEE Transactions on Vehicular Technology*, vol. 60, no. 6, pp. 2458–2470, 2011, doi: 10.1109/TVT.2011.2157186.

[15] Z. Qin, Y. Luo, W. Zhuang, Z. Pan, K. Li, and H. Peng, "Simultaneous optimization of topology, control and size for multi-mode hybrid tracked vehicles," *Applied Energy*, vol. 212, no. August 2017, pp. 1627–1641, 2018, doi: 10.1016/j.apenergy.2017.12.081.

[16] F. Ju, W. Zhuang, L. Wang, and Z. Zhang, "Optimal sizing and adaptive energy management of a novel four-wheel-drive hybrid powertrain," *Energy*, vol. 187, p. 116008, 2019, doi: 10.1016/j.energy.2019.116008.

[17] J. J. Eckert, L. C. A. Silva, E. S. Costa, F. M. Santiciolli, F. G. Dedini, and F. C. Corrêa, "Electric vehicle drivetrain optimisation," *IET Electrical Systems in Transportation*, vol. 7, no. 1, pp. 32–40, Mar. 2017, doi: 10.1049/iet-est.2016.0022.

[18] K. Deb, A. Pratap, S. Agarwal, and T. Meyarivan, "A fast and elitist multiobjective genetic algorithm: NSGA-II," *IEEE Transactions on Evolutionary Computation*, vol. 6, no. 2, pp. 182–197, Apr. 2002, doi: 10.1109/4235.996017.

[19] O. Hegazy *et al.*, "Modeling, analysis and feasibility study of new drivetrain architectures for off-highway vehicles," *Energy*, vol. 109, pp. 1056–1074, Aug. 2016, doi: 10.1016/j.energy.2016.05.001.

[20] M. Vafaeipour, D.-D. Tran, T. Geury, M. el Baghdadi, and O. Hegazy, "Application of Ant Colony Optimization for Co-Design of Hybrid Electric Vehicles," in *The Application of Ant Colony Optimization*, vol. 32, IntechOpen, 2021, pp. 137–144. doi: 10.5772/intechopen.97559.